Published in final edited form as:
Circulation. 2004 March 16; 109(10): 1284–1291. doi:10.1161/01.CIR.0000121426.43044.2B.

Aldosterone, Through Novel Signaling Proteins, Is a Fundamental Molecular Bridge Between the Genetic Defect and the Cardiac Phenotype of Hypertrophic Cardiomyopathy

Natalia Tsybouleva, MD, **Lianfeng Zhang, PhD**, **Suetnee Chen, MS**, **Rajnikant Patel, MD**, **Silvia Lutucuta, MD**, **Shintaro Nemoto, MD**, **Gilberto DeFreitas, BS**, **Mark Entman, MD**, **Blase A. Carabello, MD**, **Robert Roberts, MD**, and **A.J. Marian, MD**
Sections of Cardiology and Cardiovascular Sciences, Department of Medicine, Baylor College of Medicine and The Methodist Hospital, Houston, Tex

Abstract

Background—Human hypertrophic cardiomyopathy (HCM), the most common cause of sudden cardiac death in the young, is characterized by cardiac hypertrophy, myocyte disarray, and interstitial fibrosis. The genetic basis of HCM is largely known; however, the molecular mediators of cardiac phenotypes are unknown.

Methods and Results—We show myocardial aldosterone and aldosterone synthase mRNA levels were elevated by 4- to 6-fold in humans with HCM, whereas cAMP levels were normal. Aldosterone provoked expression of hypertrophic markers (*NPPA*, *NPPB*, and *ACTA1*) in rat cardiac myocytes by phosphorylation of protein kinase D (PKD) and expression of collagens (*COL1A1*, *COL1A2*, and *COL3A1*) and transforming growth factor-β1 in rat cardiac fibroblasts by upregulation of phosphoinositide 3-kinase (PI3K)-p100δ. Inhibition of PKD and PI3K-p110δ abrogated the hypertrophic and profibrotic effects, respectively, as did the mineralocorticoid receptor (MR) antagonist spironolactone. Spironolactone reversed interstitial fibrosis, attenuated myocyte disarray by 50%, and improved diastolic function in the cardiac troponin T (cTnT)-Q92 transgenic mouse model of human HCM. Myocyte disarray was associated with increased levels of phosphorylated β-catenin (serine 38) and reduced β-catenin–N-cadherin complexing in the heart of cTnT-Q92 mice. Concordantly, distribution of N-cadherin, predominantly localized to cell membrane in normal myocardium, was diffuse in disarrayed myocardium. Spironolactone restored β-catenin–N-cadherin complexing and cellular distribution of N-cadherin and reduced myocyte disarray in 2 independent randomized studies.

Conclusions—The results implicate aldosterone as a major link between sarcomeric mutations and cardiac phenotype in HCM and, if confirmed in additional models, signal the need for clinical studies to determine the potential beneficial effects of MR blockade in human HCM.

Keywords

cardiomyopathy; myocytes; hypertrophy

Hypertrophic cardiomyopathy (HCM) is a genetic disease characterized by unexplained cardiac and myocyte hypertrophy, interstitial fibrosis, and myocyte disarray.[1-3] Although hypertrophy and fibrosis are common to a variety of cardiovascular diseases, myocyte disarray

Reprint requests to A.J. Marian, MD, Baylor College of Medicine, Section of Cardiology, One Baylor Plaza, 519D, Houston, TX 77030. amarian@bcm.tmc.edu.

is considered the pathological hallmark of HCM. HCM is the most common cause of sudden cardiac death (SCD) in the young and a major cause of mortality and morbidity in elderly.[4] Myocyte disarray, interstitial fibrosis, and hypertrophy are considered major determinants of SCD in HCM.[5-7]

The genetic basis of HCM has been all but elucidated, with more than 150 mutations in at least 11 different sarcomeric proteins having been identified.[2,3] The primary defects induced by the genetic mutations, although diverse, directly or indirectly alter cardiac myocyte function, which leads to activation of stress-responsive trophic and mitotic factors and thus induction of hypertrophy, disarray, and interstitial fibrosis.[8] In support of this hypothesis, we have shown blockade of angiotensin II or hypertrophic signaling molecules with simvastatin markedly reduced cardiac hypertrophy and fibrosis in genetic animal models of HCM.[9,10] However, myocyte disarray, which is probably directly linked to the primary genetic defect and perhaps is fundamental to development of the overall phenotype, was unaffected. In ascertaining molecular mediators of cardiac phenotypes in HCM, we investigated aldosterone, which has been implicated in cardiac hypertrophy, interstitial fibrosis, and heart failure. Notably, overexpression of mineralocorticoid receptors (MRs), responsible for the genomic effects of aldosterone, causes cardiomyopathy in mice.[11] Similarly, cardiac-specific overexpression of 11-β-hydroxysteroid dehydrogenase-2, which increases aldosterone occupancy of the MR, leads to cardiac hypertrophy, fibrosis, and heart failure.[12] Furthermore, clinical studies in humans with heart failure, which show that blockade of MR reduces cardiovascular mortality and morbidity, emphasize the potential clinical utility of blockade of MR in cardiomyopathies.[13,14] Accordingly, we investigated the role of aldosterone in the pathogenesis of the cardiac phenotype in human HCM, delineated novel molecular mechanisms for the hypertrophic and profibrotic effects of aldosterone, and determined the effects of blockade of MR on cardiac phenotype in a transgenic mouse model of human HCM mutation.

Methods

Serum and Myocardial Aldosterone Levels in Humans With HCM

Blood was collected in the morning in sitting position from 11 patients with HCM and 8 healthy asymptomatic individuals. Aldosterone levels were determined with an enzyme competitive immunoassay, whereby aldosterone competes with horseradish peroxidase–conjugated aldosterone for the limited number of binding sites on antialdosterone serum-coated microwell plates, per instruction of the manufacturer (Diagnostic Biochem Canada Inc).

Myocardial cAMP Levels

The myocardial level of cAMP, which is known to regulate expression of the aldosterone synthase (*CYP11B2*) gene,[15] was measured by a nonacetylation enzyme immunoassay, as described by the manufacturer (Amersham Biosciences).

Isolation of Neonatal Rat Cardiac Myocytes and Fibroblasts

Neonatal rat cardiac myocytes (NRCMs) and fibroblasts (CF) were isolated from the ventricular tissue of 1- to 2-day-old neonatal rats by collagenase digestion and selective enrichment by differential centrifugation through a discontinuous Percoll gradient.[16]

Aldosterone Treatment

Cultured NRCMs and CFs were treated with 25 or 50 nmol/L aldosterone (Sigma-Aldrich Corporation), angiotensin II at a concentration of 10^{-7} mol/L as a positive control, or the MR antagonist spironolactone (100 nmol/L) at several time points. For in vivo experiments, aldosterone was dissolved in DMSO, diluted in 0.9% NaCl to 1 μmol/L concentration, and

injected intraperitoneally at 150 μL per mouse. Mice were killed at different time points after injection, and cardiac ventricular tissues were collected for the experiments.

cTnT-Q92 Transgenic Mice

The Animal Subjects Committee of Baylor College of Medicine approved the experiments. The cardiac troponin T (cTnT)-Q92 transgenic mouse model has been published previously.[9,17,18]

Reverse Transcription–Polymerase Chain Reaction

Expression levels of the molecular marker of cardiac hypertrophy, namely, *NPPA*, *NPPB*, *ACTA1*, *ATP2A2*, encoding atrial natriuretic peptide, brain natriuretic peptide, skeletal α-actin, and sarcoplasmic reticulum calcium ATPase 2, respectively, and *COL1A1*, *COL1A2*, and *COL3A1*, encoding procollagen COL1(α1), COL1(α2), and COL3(α1), respectively, were determined with specific Taqman probes and oligonucleotide primers in a 7900HT SDS unit (Applied Biosystems, Inc) and were normalized to that of GAPDH. Experiments were performed in triplicate at 3 time points of 12, 24, and 48 hours after treatment and were repeated at least 3 times.

After identification of protein kinase D (PKD) as a mediator of the hypertrophic effect of aldosterone, reverse transcription–polymerase chain reaction (RT-PCR) experiments were repeated in the presence of 100 and 500 nmol/L doses of a classic protein kinase C/PKD inhibitor, Go6976 (Calbiochem). Similarly, after identification of phosphoinositide 3-kinase (PI3K)-p110δ as a mediator of the profibrotic effects of aldosterone, RT-PCR experiments were repeated in the presence of 50 and 100 nmol/L of wortmannin (Calbiochem), a classic PI3K inhibitor.

Immunoblotting

The list of antibodies used in immunoblotting is available on request. Each set of the experiments was repeated from 3 to 5 times, and expression levels of the proteins were quantified by spot densitometry as described previously.[10] The membranes were probed with specific antibodies to detect levels of total signaling proteins, tubulin or sarcomeric actin, as controls.

Immunoprecipitation

Protein extracts were precipitated with an anti-pan cadherin antibody (delipidized whole serum, protein concentration 65 mg/mL; Sigma) and probed with rabbit anti-β-catenin antibody at 1:1000 dilution (Sigma). Signals were detected with donkey anti-rabbit Ig, horseradish peroxidase–linked whole antibody (Amersham Biosciences) by chemiluminescence.

Randomized Placebo-Controlled Spironolactone Therapy

We performed 2 independent (main and replication) placebo-controlled, randomized studies. The replication study was designed to test the findings of the primary study assuming a priori null hypothesis of no effect. Age- and gender-matched adult mutant cTnT-Q92 mice were randomized to treatment with either a placebo or spironolactone, and a third group of age- and gender-matched nontransgenic mice were included as controls (n=13 per group in the main study and n=10 in the replication studies). All mice underwent 2D and Doppler echocardiography before and after treatment. Spironolactone was dissolved in olive oil at a concentration of 10 mg/mL and injected subcutaneously at a dose of 50 $mg \cdot kg^{-1} \cdot d^{-1}$ per mouse, a dose shown to reduce myocardial fibrosis in a variety of experimental models.[19-22] The placebo group was injected with olive oil alone. After 10 weeks of therapy, mice were killed for morphometric and molecular phenotyping.

M-Mode, 2D, and Doppler Echocardiography

Transthoracic echocardiography was performed, before and after completion of spironolactone therapy, with an Acuson Sequoia Cardiac System equipped with a 15-MHz linear transducer (Acuson Co).

Morphometric Analyses

All quantification was performed in a random order by an examiner without knowledge of the experimental groups. The percentage of myocardium that showed disarray and the collagen volume fraction (CVF) were quantified in 240 fields (×400) per mouse, as described previously.[9,10] Interobserver and intraobserver variabilities of calculating the extent of myocyte disarray and fibrosis were determined in 312 fields.

To define myocyte boundary, fresh frozen thin myocardial sections were stained with a rabbit polyclonal anti-laminin antibody (Sigma) at a concentration of 1:50, and myocyte cross-sectional area (CSA) was determined by quantitative indirect immunofluorescence. The secondary antibody was Texas red streptavidin-conjugate goat anti-mouse antibody (concentration of 1:200). Nuclei were stained with Hoechst dye. The mean myocyte CSA was determined in 40 fields per mouse in 5 mice per group (≈2500 myocytes for each group).

Statistical Methods

Differences in variables among nontransgenic, placebo, and spironolactone groups were compared by ANOVA, followed by Bartlett's test for the homogeneity of variances. Variables with unequal SDs, such as CVF, were compared by the nonparametric Kruskal-Wallis test. Differences between final and baseline values in each group were compared by paired *t* test.

Results

Myocardial Aldosterone and *CYP11B2* Levels in Humans

HCM patients comprised 6 males and 5 females with a mean±SD age of 55.6±16.6 years, septal thickness of 2.03±0.49 cm, left ventricular (LV) mass of 332.8±93.8 g, LV ejection fraction of 68.9±5.8%, and LV outflow tract gradient of 54.4±23.8 mm Hg. They were symptomatic for dyspnea, with a mean New York Heart Association functional class of 1.6±0.98. Myocardial tissues were collected during surgical myomectomy or at postmortem examination. The control myocardial tissues were age- and gender-matched normal donor hearts not used for cardiac transplantation. Tissues were frozen in liquid nitrogen and stored at −135°C. Mean serum aldosterone levels were not significantly different between HCM and control subjects (Figure 1A). In contrast, myocardial aldosterone levels were increased by 4.5-fold in HCM (Figure 1B). Concordantly, expression levels of *CYP11B2* mRNA in the heart, quantified by RT-PCR, were increased by 6.9-fold (Figure 1C).

Myocardial cAMP Levels

Myocardial cAMP levels were not significantly different between HCM patients and controls (12.1±6.8 versus 8.7±10.8 fmol/mg, respectively; P=0.552).

Hypertrophic and Profibrotic Effects of Aldosterone

Treatment of NRCMs with 2 doses of aldosterone provoked significant expression of *NPPA*, *NPPB*, and *ACTA1* at 12, 24, and 48 hours (Figure 2) and modestly reduced expression levels of *ATP2A2*. Similarly, treatment of cultured CFs with 2 doses of aldosterone significantly increased expression levels of *COL1A1*, *COL1A2*, and *COL3A1* mRNAs at 24 and 48 hours (Figure 3). Spironolactone blocked the hypertrophic and profibrotic effects of aldosterone in cultured myocytes and fibroblasts (Figures 2 and 3). Concordantly, expression levels of

transforming growth factor (TGF)-β1, a major profibrotic factor, were also increased in cultured CFs after 30 and 60 minutes of treatment with aldosterone and were blocked by spironolactone (Figure 4).

Signal Transducers of Hypertrophic and Fibrotic Effects of Aldosterone

Because classic PKCs are implicated in the mediation of aldosterone signaling,[23] we investigated activation of PKC isoforms in NRCMs and CFs after treatment with aldosterone. The most notable effect was phosphorylation of PKD, which was serine residue specific and cyclic (Figure 5A). Aldosterone phosphorylated PKD at serine 916, which peaked initially at 60 minutes. Aldosterone had no major effect on levels of serine 744 to 748 phosphorylated PKD or total PKD. In contrast to NRCMs, aldosterone had no significant effect on levels of S916-phospho-PKD or S744–748-phospho-PKD in CFs (Figure 5B). Increased PKD phosphorylation was also confirmed in vivo in explanted hearts after treatment of adult mice with aldosterone, with increased expression levels of S916-phospho-PKD in cardiac myocytes (Figure 5C) but not in fibroblasts (data not shown). Other notable changes were increased levels of phosphorylated p42/44 extracellular signal-regulated kinases and levels of calcineurin in NRCMs after treatment with aldosterone, in accordance with published data.[24,25]

In the absence of a discernible effect of aldosterone on PKD activation in CFs, and given that the PI3K pathway is implicated in interstitial fibrosis,[26] we determined changes in expression levels of the PI3K components after treatment of CFs with aldosterone. Expression of PI3K-p110δ was increased in a time-dependent manner, peaking at 60 minutes, whereas levels of other known components were largely unchanged (Figure 5D). Similarly, expression levels of PI3K-p110δ were increased in CFs isolated from myocardium of adult mice treated with intraperitoneal injection of aldosterone but not in myocytes isolated from the same mice (Figure 5E).

To determine whether phosphorylation of PKD was responsible for the hypertrophic response to aldosterone, cultured NRCMs were treated with aldosterone in the presence of 2 different concentrations of Go6976, an inhibitor of classic PKC/PKD, and expression levels of markers of cardiac hypertrophy were determined by RT-PCR. Treatment of cultured NRCMs with Go6976 completely abrogated the hypertrophic response to aldosterone (Figure 6). Similarly, treatment of cultured CFs with 2 concentrations of wortmannin, a PI3K inhibitor, abolished induction of expression of procollagen mRNAs by aldosterone (Figure 6).

Cardiac Phenotype in Adult cTnT-Q92 Transgenic Mice

Cardiac phenotype in the cTnT-Q92 mice was as published previously.[9,17] Heart weight/body weight ratio was smaller by 15% in a total of 33 mutant mice analyzed in the present study compared with nontransgenic littermates; myocyte disarray constituted ≈20% of the myocardium, and CVF was increased by 3-fold. The intraobserver and interobserver variabilities in determining CVF were 1.25% and 1.8%, and for disarray, they were 2.3% and 3.6%, respectively.

Myocardial levels of aldosterone were 0.11±0.02 and 0.08±0.04 pg/g of LV tissue in cTnT-Q92 and nontransgenic mice, respectively (P=0.17). Serum levels of aldosterone were not significantly different between cTnT-Q92 and non-transgenic mice.

Effects of Spironolactone on Cardiac Phenotype in cTnT-Q92 Transgenic Mice

The mean age, male/female ratio, heart rate, and body weight were not significantly different among the nontransgenic, placebo, and spironolactone groups in the main and replication studies (data not shown). Results of the main study, shown in the Table, were notable for a smaller heart weight/body weight ratio in the spironolactone group. The extent of myocyte

disarray, determined in a total of 3960 fields per group, was reduced by 50% in the spironolactone versus the placebo group. Moreover, CVF was reduced to normal levels in the spironolactone group. Myocyte CSA was not significantly different between spironolactone and placebo groups but was smaller in transgenic than in nontransgenic mice. Overall, spironolactone had no significant effect on heart rate, body weight, and echocardiographic indices of ventricular size or function, with the exception of a significant improvement of mitral inflow E/A ratio.

The results in the replication study, scored in a twice larger number of myocardial sections, were concordant with the results of the main randomized study and showed a 50% reduction in the extent of myocyte disarray in the spironolactone versus the placebo group (8.3±2.9% versus 17.5±9.1%, respectively, $P< 0.001$) and complete normalization of CVF (6.7±4.9 versus 1.4%±0.4, $P=0.001$).

Disrupted Localization and Complexing of N-Cadherin–β-Catenin in Disarrayed Myocardium

We tested the integrity of cadherin-mediated myocyte-myocyte adhesion at the adherens junction (AJ), a potential mechanism for myocyte disarray, by determining expression levels and intracellular distribution of N-cadherin and phosphorylated-β-catenin (serine 37) in the heart of cTnT-Q92 mice. Confocal microscopy showed predominant localization of N-cadherin to myocyte membranes in nontransgenic hearts, whereas its distribution was diffuse and less restricted to AJ in disarrayed myocardium (Figure 7A). Treatment with spironolactone partially restored the distribution of N-cadherin to AJ, in accordance with the reduction in myocyte disarray. Furthermore, levels of S37-phospho-β-catenin were increased by ≈2-fold, whereas levels of N-cadherin were unchanged (Figure 7B). Coimmunoprecipitation experiments (Figure 7C) showed reduced affinity of S37-phospho-β-catenin for N-cadherin, which provides further evidence for destabilized AJ in disarrayed areas. Treatment with spironolactone normalized levels of S37-phospho-β-catenin and β-catenin/cadherin complex formation.

Discussion

We explored the molecular mechanisms that link the genetic defect to the cardiac phenotype in HCM, with a particular focus on myocyte disarray and interstitial fibrosis. We provide several lines of evidence to implicate aldosterone in the pathogenesis of cardiac hypertrophy, fibrosis, and disarray in HCM, including elevated myocardial aldosterone and aldosterone synthase mRNA levels in patients with HCM. Aldosterone provoked expression of cardiac hypertrophic and profibrotic responses in cultured myocytes and fibroblasts through activation of PKD and increased expression of P13K-p110δ in cardiac myocytes and fibroblasts, respectively. Blockade of PKD and PI3K-p110δ abrogated the hypertrophic and profibrotic effects of aldosterone. We also performed 2 independent studies and showed that blockade of MR in a genetically engineered mouse model of HCM mutation normalized myocardial collagen content and attenuated myocyte disarray, phenotypes associated with SCD and heart failure in HCM[7,27] and improvement in diastolic function. Finally, we provide evidence implicating impaired N-cadherin–mediated myocyte-myocyte attachment, as a consequence of phosphorylation of β-catenin, in the pathogenesis of myocyte disarray, the hallmark of HCM. Collectively, the results in human hearts, cultured cells, and a genetic animal model of HCM identify aldosterone as a fundamental molecular link between sarcomeric gene mutations and cardiac phenotypes in HCM. These results, if confirmed in additional studies and for other HCM-causing mutations, in conjunction with the results of recent clinical studies showing the beneficial effects of blockade of MR in heart failure[13,14] illustrate the need for clinical studies in humans to determine the potential beneficial effects of blockade of MR in HCM.

Aldosterone, discovered 50 years ago,[28] is known primarily for its effects on sodium transport in renal tubules, whereas its direct effects on cardiac structure and function are largely

unrecognized. The observed increased myocardial aldosterone levels in patients with HCM is in accordance with the results of recent studies showing extraadrenal gland synthesis of aldosterone, including studies in cardiac myocytes and fibroblasts and the myocardium of patients with heart failure.[19,27,29,30] In the adrenal glands and cultured cells, expression of *CYP11B2* is regulated by a diverse array of factors, including angiotensin II,[31] cAMP,[15] 12-lipoxygenase,[32] PKC isoforms,[33,34] and calmodulin-dependent protein kinases.[35] These factors, alone or in combination, are plausible candidates to affect expression of *CYP11B2* in HCM hearts. In the present study, myocardial cAMP levels and lipid peroxide levels, an overall index of oxidative stress, were not significantly elevated (data not shown), perhaps because they were less stable in the stored tissue. The molecular mechanisms that regulate expression of *CYP11B2* and production of aldosterone in the heart in general and in HCM in particular remain to be established.

Aldosterone imparts a diverse array of biological effects comprising genomic (slow) and nongenomic (rapid) components, including but not limited to changes in the intracellular calcium concentration,[36] Na^+/H^+ exchanger,[37] and activation of extracellular signal-regulated kinases p22/44,[25] phospholipase C,[23] and calcineurin.[24] The present findings implicate PKD and PI3K-p110δ as the molecular mediators of cardiac hypertrophic and profibrotic effects and provide for novel mechanisms for the actions of aldosterone. Notably, neither PKD nor PI3K-p110δ has been implicated previously in cardiac hypertrophy and fibrosis. The results, in conjunction with the existing data implicating PKD in cell proliferation, invasiveness, apoptosis, and cellular morphology (reviewed in Rykx et al[38]), render PKD as an attractive molecular target in cardiomyopathies. Similarly, identification of PI3K-p110δ as an effector for aldosterone and its involvement in cardiac fibrosis has broader clinical implications, because fibrosis is a common pathological phenotype of cardiovascular diseases and is considered a predictor of cardiac arrhythmias and SCD.[39] Furthermore, because p110δ is also implicated in the regulation of actin cytoskeleton dynamics and cell migration,[40] upregulation of its expression by aldosterone could also contribute to regulation of cardiac myocyte organization, ie, myocyte disarray.

The present data indicate that impaired myocyte-myocyte attachment at AJ because of impaired phospho-β-catenin and N-cadherin complexing is responsible, at least in part, for myocyte disarray in HCM. The extracellular domains of cadherins form the intercellular bonds between adjacent myocytes, and the cytoplasmic domains attach to cytoskeletal actin through β-catenin and other effector proteins. The integrity of AJ is essential for the proper alignment of myocytes. Alternative mechanisms for the observed reduction of myocyte disarray could include normalization of interstitial fibrosis and thus restoration of myocardial architecture. It is also possible that increased extracellular matrix proteins in HCM, by activating the integrin/wnt signaling pathways, affect the integrity of the β-catenin–cadherin–axin complex and thus myocyte morphology and arrangement.[41] Accordingly, multiple interdependent mechanisms could be involved in the pathogenesis of myocyte disarray in HCM and its attenuation by spironolactone.

The results of 2 independent, randomized, placebo-controlled studies with spironolactone in cTnT-Q92 mice were concordant and in accordance with the mechanisms delineated for the effects of aldosterone in cell culture studies. Detailed quantification of the extent of myocyte disarray in the primary and replication studies, scored in a total of 11 880 microscopic fields in 23 mice per group, showed a 50% reduction with spironolactone (4.2±1.8 in nontransgenic mice, 19.3±8.0 in the placebo mice, and 9.5±3.0 in the spironolactone group; $P<0.001$), which is beyond the 3% to 4% interindividual and intraindividual variabilities. Reversal of interstitial fibrosis with spironolactone is also in agreement with the results of previous observations in other animal models of cardiovascular disorders.[19-22,29,42] As is often the case in humans with cTnT mutations,[43,44] the cTnT-Q92 mice do not exhibit cardiac hypertrophy.[17,45] Therefore,

the impact of spironolactone on potential regression of cardiac hypertrophy in vivo could not be assessed. Treatment with spironolactone further reduced the heart weight/body weight ratio (3.5±0.5 versus 4.0±0.7 in the placebo group, $P<0.001$). Because myocyte CSA did not change, the reduction in heart weight/body weight ratio in the spironolactone group most likely represents the reduction in interstitial fibrosis. Because human patients with the cTnT-Q92 mutation exhibit extensive myocyte disarray, a potential risk factor for SCD,[44] the findings raise the possibility of reducing the risk of SCD in HCM through blockade of MR, a hypothesis that awaits testing in humans.

In summary, the present data implicate aldosterone in the pathogenesis of the cardiac phenotype in HCM and identify novel mechanisms for its hypertrophic and profibrotic effects by implicating PKD and PI3K-p110δ, respectively. Our data also implicate impaired N-cadherin–β-catenin complexing at AJ as a mechanism for myocyte disarray, the pathological hallmark of HCM. Finally, our data establish the reversibility of cardiac phenotypes through blockade of MR. These findings, in the absence of a specific therapy for human HCM, if confirmed in additional studies, emphasize the need for clinical studies to determine potential salutary effects of blockade of MR in human patients with HCM.

Acknowledgments

This study was supported by grants from the National Heart, Lung, and Blood Institute, Specialized Centers of Research (P50-HL42267-01) and R01-HL-68884.

References

1. Maron BJ. Hypertrophic cardiomyopathy: a systematic review. JAMA 2002;287:1308–1320. [PubMed: 11886323]
2. Marian AJ, Roberts R. The molecular genetic basis for hypertrophic cardiomyopathy. J Mol Cell Cardiol 2001;33:655–670. [PubMed: 11273720]
3. Fatkin D, Graham RM. Molecular mechanisms of inherited cardiomyopathies. Physiol Rev 2002;82:945–980. [PubMed: 12270949]
4. Maron BJ, Shirani J, Poliac LC, et al. Sudden death in young competitive athletes: clinical, demographic, and pathological profiles. JAMA 1996;276:199–204. [PubMed: 8667563]
5. Shirani J, Pick R, Roberts WC, et al. Morphology and significance of the left ventricular collagen network in young patients with hypertrophic cardiomyopathy and sudden cardiac death. J Am Coll Cardiol 2000;35:36–44. [PubMed: 10636256]
6. Spirito P, Bellone P, Harris KM, et al. Magnitude of left ventricular hypertrophy and risk of sudden death in hypertrophic cardiomyopathy. N Engl J Med 2000;342:1778–1785. [PubMed: 10853000]
7. Varnava AM, Elliott PM, Mahon N, et al. Relation between myocyte disarray and outcome in hypertrophic cardiomyopathy. Am J Cardiol 2001;88:275–279. [PubMed: 11472707]
8. Marian AJ. Pathogenesis of diverse clinical and pathological phenotypes in hypertrophic cardiomyopathy. Lancet 2000;355:58–60. [PubMed: 10615904]
9. Lim DS, Lutucuta S, Bachireddy P, et al. Angiotensin II blockade reverses myocardial fibrosis in a transgenic mouse model of human hypertrophic cardiomyopathy. Circulation 2001;103:789–791. [PubMed: 11171784]
10. Patel R, Nagueh SF, Tsybouleva N, et al. Simvastatin induces regression of cardiac hypertrophy and fibrosis and improves cardiac function in a transgenic rabbit model of human hypertrophic cardiomyopathy. Circulation 2001;104:317–324. [PubMed: 11457751]
11. Le Menuet D, Isnard R, Bichara M, et al. Alteration of cardiac and renal functions in transgenic mice overexpressing human mineralocorticoid receptor. J Biol Chem 2001;276:38911–38920. [PubMed: 11495902]
12. Qin W, Rudolph AE, Bond BR, et al. Transgenic model of aldosterone-driven cardiac hypertrophy and heart failure. Circ Res 2003;93:69–76. [PubMed: 12791709]

13. Pitt B, Remme W, Zannad F, et al. Eplerenone, a selective aldosterone blocker, in patients with left ventricular dysfunction after myocardial infarction. N Engl J Med 2003;348:1309–1321. [PubMed: 12668699]
14. Pitt B, Zannad F, Remme WJ, et al. The effect of spironolactone on morbidity and mortality in patients with severe heart failure: Randomized Aldactone Evaluation Study Investigators. N Engl J Med 1999;341:709–717. [PubMed: 10471456]
15. Bassett MH, Zhang Y, White PC, et al. Regulation of human CYP11B2 and CYP11B1: comparing the role of the common CRE/Ad1 element. Endocr Res 2000;26:941–951. [PubMed: 11196473]
16. Malhotra R, Brosius FC III. Glucose uptake and glycolysis reduce hypoxia-induced apoptosis in cultured neonatal rat cardiac myocytes. J Biol Chem 1999;274:12567–12575. [PubMed: 10212235]
17. Oberst L, Zhao G, Park JT, et al. Dominant-negative effect of a mutant cardiac troponin T on cardiac structure and function in transgenic mice. J Clin Invest 1998;102:1498–1505. [PubMed: 9788962]
18. Solaro RJ, Varghese J, Marian AJ, et al. Molecular mechanisms of cardiac myofilament activation: modulation by pH and a troponin T mutant R92Q. Basic Res Cardiol. In press
19. Silvestre JS, Heymes C, Oubenaissa A, et al. Activation of cardiac aldosterone production in rat myocardial infarction: effect of angiotensin II receptor blockade and role in cardiac fibrosis. Circulation 1999;99:2694–2701. [PubMed: 10338465]
20. Fiebeler A, Schmidt F, Muller DN, et al. Mineralocorticoid receptor affects AP-1 and nuclear factor-kappab activation in angiotensin II-induced cardiac injury. Hypertension 2001;37:787–793. [PubMed: 11230374]
21. Brilla CG, Matsubara LS, Weber KT. Antifibrotic effects of spironolactone in preventing myocardial fibrosis in systemic arterial hypertension. Am J Cardiol 1993;71:12A–16A.
22. Miric G, Dallemagne C, Endre Z, et al. Reversal of cardiac and renal fibrosis by pirfenidone and spironolactone in streptozotocin-diabetic rats. Br J Pharmacol 2001;133:687–694. [PubMed: 11429393]
23. Christ M, Meyer C, Sippel K, et al. Rapid aldosterone signaling in vascular smooth muscle cells: involvement of phospholipase C, diacyl-glycerol and protein kinase C alpha. Biochem Biophys Res Commun 1995;213:123–129. [PubMed: 7639725]
24. Takeda Y, Yoneda T, Demura M, et al. Calcineurin inhibition attenuates mineralocorticoid-induced cardiac hypertrophy. Circulation 2002;105:677–679. [PubMed: 11839620]
25. Stockand JD, Meszaros JG. Aldosterone stimulates proliferation of cardiac fibroblasts by activating Ki-RasA and MAPK1/2 signaling. Am J Physiol Heart Circ Physiol 2003;284:H176–H184. [PubMed: 12388314]
26. Ricupero DA, Poliks CF, Rishikof DC, et al. Phosphatidylinositol 3-kinase-dependent stabilization of alpha1(I) collagen mRNA in human lung fibroblasts. Am J Physiol Cell Physiol 2001;281:C99–C105. [PubMed: 11401831]
27. Silvestre JS, Robert V, Heymes C, et al. Myocardial production of aldosterone and corticosterone in the rat: physiological regulation. J Biol Chem 1998;273:4883–4891. [PubMed: 9478930]
28. Williams JS, Williams GH. 50th anniversary of aldosterone. J Clin Endocrinol Metab 2003;88:2364–2372. [PubMed: 12788829]
29. Delcayre C, Silvestre JS, Garnier A, et al. Cardiac aldosterone production and ventricular remodeling. Kidney Int 2000;57:1346–1351. [PubMed: 10760065]
30. Mizuno Y, Yoshimura M, Yasue H, et al. Aldosterone production is activated in failing ventricle in humans. Circulation 2001;103:72–77. [PubMed: 11136688]
31. Ye P, Kenyon CJ, MacKenzie SM, et al. Regulation of aldosterone synthase gene expression in the rat adrenal gland and central nervous system by sodium and angiotensin II. Endocrinology 2003;144:3321–3328. [PubMed: 12865309]
32. Gu J, Wen Y, Mison A, et al. 12-Lipoxygenase pathway increases aldosterone production, 3′,5′-cyclic adenosine monophosphate response element-binding protein phosphorylation, and p38 mitogen-activated protein kinase activation in H295R human adrenocortical cells. Endocrinology 2003;144:534–543. [PubMed: 12538614]
33. LeHoux JG, Dupuis G, Lefebvre A. Control of CYP11B2 gene expression through differential regulation of its promoter by atypical and conventional protein kinase C isoforms. J Biol Chem 2001;276:8021–8028. [PubMed: 11115506]

34. Sato A, Liu JP, Funder JW. Aldosterone rapidly represses protein kinase C activity in neonatal rat cardiomyocytes in vitro. Endocrinology 1997;138:3410–3416. [PubMed: 9231795]
35. Condon JC, Pezzi V, Drummond BM, et al. Calmodulin-dependent kinase I regulates adrenal cell expression of aldosterone synthase. Endocrinology 2002;143:3651–3657. [PubMed: 12193581]
36. Estrada M, Liberona JL, Miranda M, et al. Aldosterone and testosterone-mediated intracellular calcium response in skeletal muscle cell cultures. Am J Physiol Endocrinol Metab 2000;279:E132–E139. [PubMed: 10893332]
37. Gekle M, Freudinger R, Mildenberger S, et al. Rapid activation of Na+/H+-exchange in MDCK cells by aldosterone involves MAP-kinase ERK1/2. Pflugers Arch 2001;441:781–786. [PubMed: 11316261]
38. Rykx A, De Kimpe L, Mikhalap S, et al. Protein kinase D: a family affair. FEBS Lett 2003;546:81–86. [PubMed: 12829240]
39. Assayag P, Carre F, Chevalier B, et al. Compensated cardiac hypertrophy: arrhythmogenicity and the new myocardial phenotype, I: fibrosis. Cardiovasc Res 1997;34:439–444. [PubMed: 9231026]
40. Sawyer C, Sturge J, Bennett DC, et al. Regulation of breast cancer cell chemotaxis by the phosphoinositide 3-kinase p110delta. Cancer Res 2003;63:1667–1675. [PubMed: 12670921]
41. Frame S, Cohen P. GSK3 takes centre stage more than 20 years after its discovery. Biochem J 2001;359:1–16. [PubMed: 11563964]
42. Brown L, Duce B, Miric G, et al. Reversal of cardiac fibrosis in deoxy-corticosterone acetate-salt hypertensive rats by inhibition of the renin-angiotensin system. J Am Soc Nephrol 1999;10(suppl 11):S143–S148. [PubMed: 9892155]
43. Watkins H, McKenna WJ, Thierfelder L, et al. Mutations in the genes for cardiac troponin T and alpha-tropomyosin in hypertrophic cardiomyopathy. N Engl J Med 1995;332:1058–1064. [PubMed: 7898523]
44. Varnava AM, Elliott PM, Baboonian C, et al. Hypertrophic cardiomyopathy: histopathological features of sudden death in cardiac troponin T disease. Circulation 2001;104:1380–1384. [PubMed: 11560853]
45. Tardiff JC, Hewett TE, Palmer BM, et al. Cardiac troponin T mutations result in allele-specific phenotypes in a mouse model for hypertrophic cardiomyopathy. J Clin Invest 1999;104:469–481. [PubMed: 10449439]

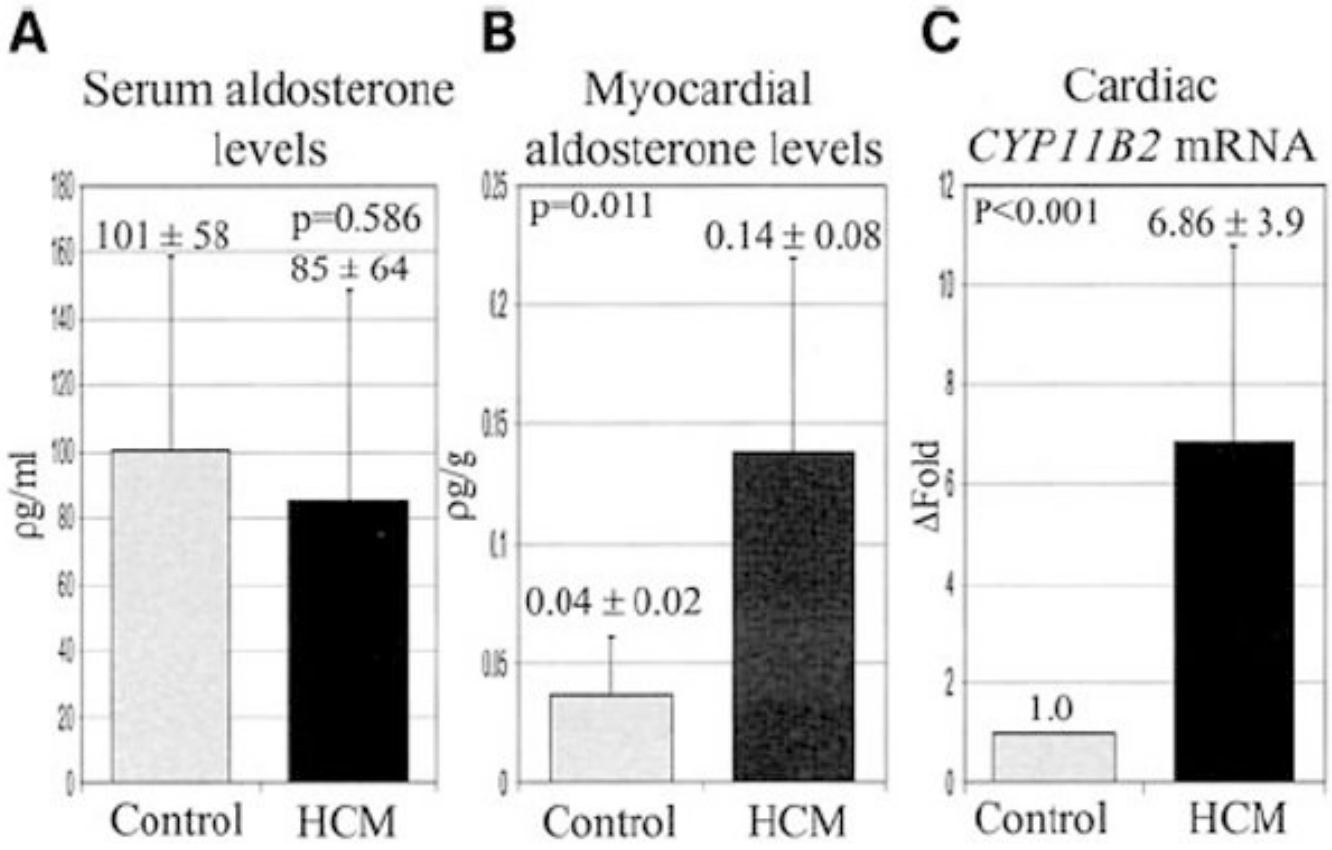

Figure 1.

Aldosterone levels in HCM. Serum (A) and myocardial (B) aldosterone levels in patient with HCM (n=8) and controls (n=11). C, Relative expression levels of *CYP11B2* mRNA in HCM (n=8) compared with controls (n=4).

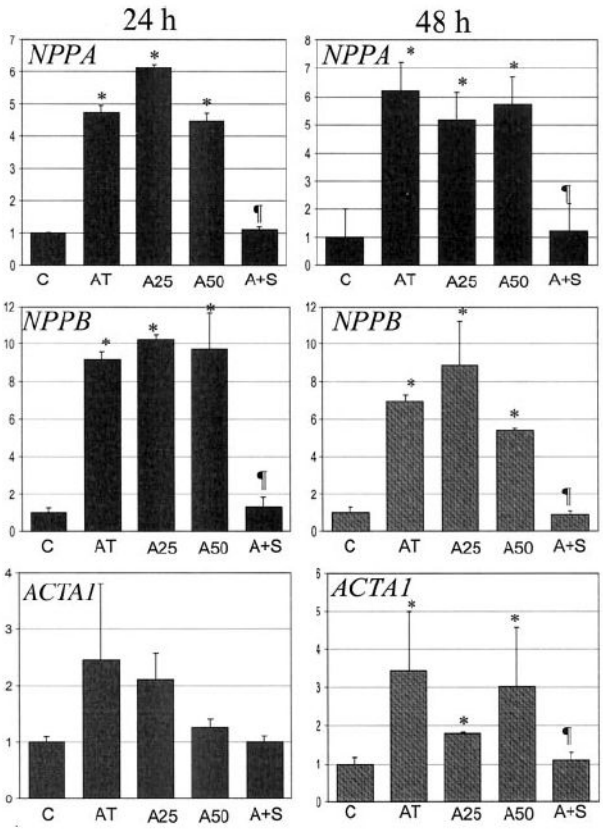

Figure 2.

Hypertrophic effect of aldosterone. Relative expression levels of mRNAs for atrial natriuretic peptide (*NPPA*), brain natriuretic peptide (*NPPB*), and skeletal α-actin (*ACTA1*) at 24 and 48 hours after treatment of cardiac myocytes with 2 doses of aldosterone (12-hour data not shown). C indicates control myocytes; AT, angiotensin II; A25 and A50, myocytes treated with aldosterone 25 and 50 nmol/L, respectively; A+S, myocytes treated with aldosterone 50 nmol/L in presence of spironolactone 0.5 μmol/L. *P<0.05 vs C; ¶P<0.05 vs A50.

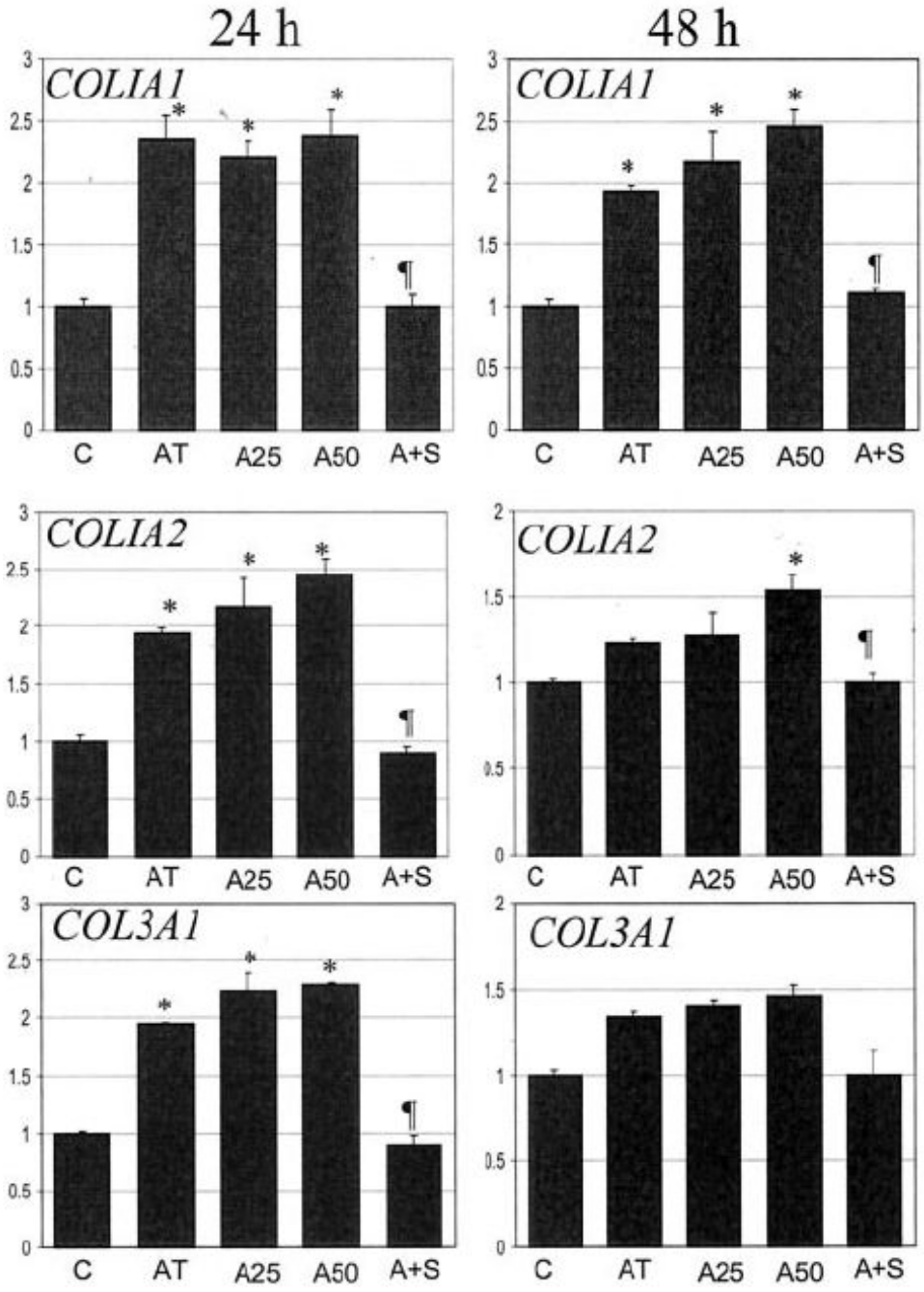

Figure 3.
Profibrotic effect of aldosterone. Relative expression levels of mRNAs for 3 main cardiac collagen genes at 24 and 48 hours after treatment of cardiac fibroblasts with aldosterone are shown. Abbreviations and symbols as in Figure 2.

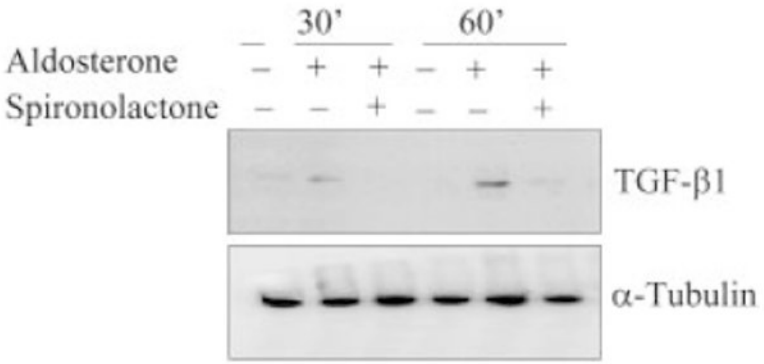

Figure 4.

Induction of expression of TGF-β1 with aldosterone in cardiac fibroblasts. Top, Induction of expression of TGF-β1 after 30 and 60 minutes of treatment with aldosterone 50 nmol/L and its blockade with spironolactone. Bottom (blot), Expression levels of α-tubulin, control for protein loading conditions.

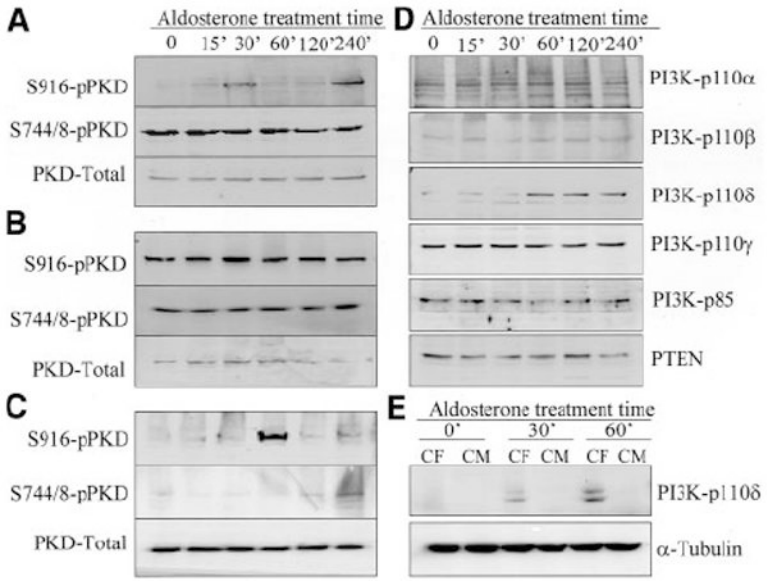

Figure 5.

Molecular mediators of aldosterone signaling in cardiac myocytes and fibroblasts. A, Immunoblot showing expression levels of serine 916 and serine 744 to 748 phosphorylated (p) and total PKD in cardiac myocytes treated with aldosterone at 6 time points. B, Expression levels of phosphorylated (p) and total PKD proteins in cardiac fibroblasts treated with aldosterone. C, Expression levels of phosphorylated (p) and total PKD proteins in mice hearts treated with aldosterone. D, Expression levels of PI3K signaling molecules and PTEN (phosphatase and tensin homolog deleted on chromosome 10) in cultured cardiac fibroblasts treated with aldosterone at 6 different time points. E, Expression of PI3K-p110*δ* in cardiac myocytes (CM) and fibroblasts (CF) isolated from hearts of mice treated with aldosterone.

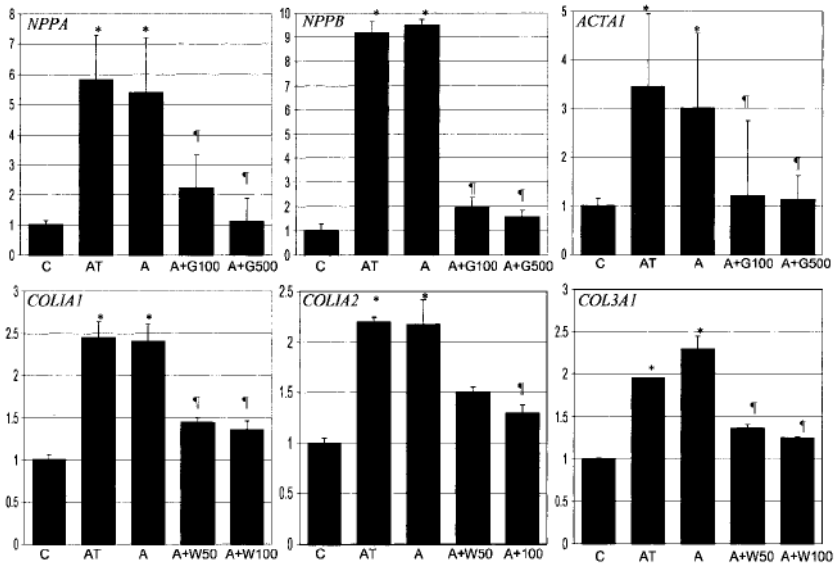

Figure 6.

Inhibition of cardiac hypertrophic and profibrotic responses of aldosterone. Top panels represent relative expression levels of 3 cardiac hypertrophic markers, as described in Figure 2. C indicates control myocytes; AT, angiotensin II; A, aldosterone; and A+G100 and A+G500, myocytes treated with aldosterone and Go6976 100 or 500 nmol/L, respectively. Bottom panels show inhibition of induction of expression of 3 major cardiac collagen genes in cardiac fibroblasts. Abbreviations are as above, except CFs were used and W50 and W100 denote fibroblasts treated with aldosterone and wortmannin 50 and 100 nmol/L, respectively. *P<0.05 vs C; ¶P<0.05 vs aldosterone.

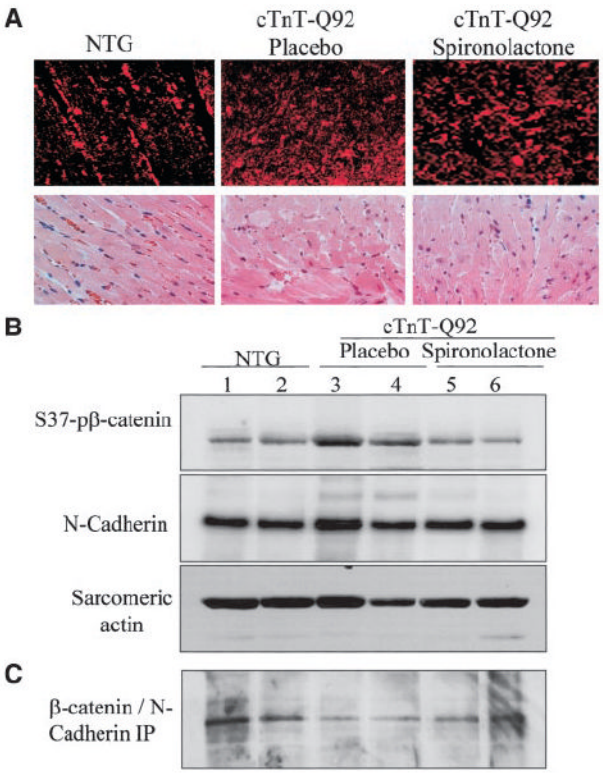

Figure 7.

Molecular basis for myocyte disarray and its attenuation with spironolactone. A, Confocal micrographs showing distribution of N-cadherin in hearts of nontransgenic (NTG) mice and cTnT-Q92 mice treated either with placebo or spironolactone. Lower panels show hematoxylin-and-eosin–stained thin sections of myocardium in experimental groups. B, Immunoblots depicting expression levels of serine 37-phosphorylated *β*-catenin in NTG, placebo, and spironolactone groups (upper panel); middle panel depicts expression levels of N-cadherin in experimental groups; and lower panel represents expression levels of sarcomeric actin, control for protein loading control. C, Representative immunoblot showing expression levels of *β*-catenin after immunoprecipitation with anti–N-cadherin antibody. IP indicates intraperitoneal.

Table

Effects of Spironolactone on Cardiac Structure and Function in cTnT-Q92 Mice

		cTnT-Q92			
	Nontransgenic Mice	Placebo	Spironolactone	*P**	*P*
Heart/body weight ratio, g/mg	4.93±0.65	3.94±0.54	3.43±0.27	0.008	<0.001
CVF, %	2.35±0.7	6.41±6.04	2.84±0.91	0.001	0.01
Myocyte disarray, %	4.77±1.6	20.68±7.2	10.23±3.1	<0.001	<0.001
Myocyte CSA, mm^2†	499.6±49.3	411.0±26.6	419±27.0	0.617	0.004
Echocardiographic parameters					
IVST, mm					
Baseline	0.75±0.09	0.77±0.05	0.72±0.06	0.020	0.16
Follow-up	0.72±0.05	0.73±0.08	0.68±0.09	0.222	0.48
PWT, mm					
Baseline	0.78±0.10	0.79±0.05	0.76±0.08	0.155	0.47
Follow-up	0.73±0.05	0.75±0.07	0.75±0.05	0.819	0.85
LVEDD, mm					
Baseline	4.1±0.3	4.0±0.3	4.0±0.3	0.745	0.47
Follow-up	4.3±0.35	4.1±0.29	3.9±0.21	0.093	0.008
LVESD, mm					
Baseline	2.9±0.33	2.3±0.37	2.3±0.32	0.658	<0.001
Follow-up	3.1±0.40	2.5±0.34	2.3±0.26	0.287	<0.001
FS, %					
Baseline	30.4±3.8	43.1±7.1	41.3±5.9	0.329	<0.001
Follow-up	28.9±4.9	39.3±5.9	39.8±4.3	0.510	<0.001
LV ejection fraction, %					
Baseline	64.3±6.2	79.1±6.9	78.0±5.9	0.457	<0.001
Follow-up	61.6±6.2	76.6±6.4	76.4±5.1	0.722	<0.001
Aortic ejection time, ms					
Baseline	52.8±3.7	60.9±4.0	60.9±7.4	0.992	0.001
Follow-up	53.1±5.7	65.0±9.8	63.6±6.8	0.709	0.001
E/A ratio					
Baseline	2.93±1.12	1.83±0.60	2.48±1.06	0.079	0.04
Follow-up	2.82±0.93	1.95±0.35	3.21±1.31‡	0.006	0.02

IVST indicates interventricular septal thickness; PWT, posterior wall thickness; LVEDD, LV end-diastolic dimension; LVESD, LV end-systolic dimension; FS, fractional shortening; and E/A ratio, ratio of mitral inflow early to late velocities.

n=13 in each group, except where noted. *P* values in the right column are derived by comparison of variables among the 3 groups by ANOVA or Kruskal-Wallis test.

* *P* between placebo and spironolactone groups only.

† n=5 mice per group.

‡ *P*=0.07 follow-up compared with baseline.